Macromolecules **2004,** *37,* 8123−8127

Secondary Relaxation of the Johari−Goldstein Kind in Alkyl Nanodomains

K. L. Ngai

Max-Planck-Institut für Physik Komplexer Systeme, Nöthnitzer Strasse 38,
D-01187 Dresden, Germany, and Naval Research Laboratory, Washington, D.C. 20375-5320

M. Beiner*

Fachbereich Physik, Universität Halle, D-06099 Halle (Saale), Germany

Received July 5, 2004; Revised Manuscript Received August 13, 2004

ABSTRACT: Previously it was shown by experiments that nanophase separation of incompatible main- and side-chain parts occurs in higher poly(*n*-alkyl acrylates) (P*n*AA) and poly(*n*-alkyl methacrylates) (P*n*AMA). Alkyl groups of different monomeric units of the polymer aggregate in the melt and form self-assembled alkyl nanodomains with a typical size of 0.5−2 nm. A polyethylene-like glass transition occurs within the alkyl nanodomains. We revisit the relaxation data and suggest that an unresolved Johari−Goldstein secondary relaxation is present in addition to the primary α-relaxation of this polyethylene-like glass transition. The ratio of the relaxation times of the two processes is consistent with the weakly cooperative nature of the α-relaxation, already indicated by its low steepness (fragility) index.

1. Introduction

Nanophase separation of incompatible main- and side-chain parts is a general phenomenon in amorphous side-chain polymers with long alkyl groups. This property was shown[1,2] by X-ray scattering and relaxation spectroscopy data acquired from higher members of the poly(*n*-alkyl acrylates) and poly(*n*-alkyl methacrylates) that alkyl groups aggregate in the melt and form self-assembled alkyl nanodomains with a typical size of 0.5−2 nm. A comparison with data for other polymer series having alkyl groups,[1] including poly(di-*n*-alkyl itaconates),[3] hairy rod polyimides,[4] and poly(alkylbenzimidazol-*alt*-thiophene),[5] reveals that the alkyl nanodomain size and dynamics are mainly determined by the number, *C*, of alkyl carbon atoms per side chain and depends slightly on the microstructure of the main chain. A polyethylene-like glass transition called α_{PE} within the alkyl nanodomains has been observed. The results described for different series of side-chain polymers support the idea[6] that nanophase separation is a general phenomenon in materials that consist of molecules with incompatible parts.

In this work we revisit the experimental relaxation data[1,2] of the α_{PE} process within the alkyl nanodomains in the poly(*n*-alkyl acrylates) and poly(*n*-alkyl methacrylates) series for $C \geq 4$. While the α_{PE} process in the higher members of both series ($C > 6$) shows truly properties of a cooperative polyethylene-like glass transition, the nanodomains in $C = 4$ have sizes significantly smaller than the cooperativity length scale,[1] and the α_{PE} process therein is expected to have cooperativity all but removed. Normally, the supposedly universal Johari−Goldstein (JG) β-relaxation[7−11] is the precursor of the cooperative α-relaxation. However, in the absence of cooperativity, the α-relaxation and the JG β-relaxation should become one and the same process. Therefore, the α_{PE} process in $C = 4$ can be identified as the JG relaxation of the alkyl nanodomains (β_{PE}) in $C > 4$. With this identification, the ratio of relaxation time of the α_{PE} process to that of the corresponding JG relaxation (β_{PE}) is known near $T_g(\alpha_{\mathrm{PE}})$, and can be used via the coupling model[12−16] as an independent verification of the weak cooperativity of the glass transition within the nanodomain in $C > 4$ and to predict the Kohlrausch exponents of the α_{PE} process.

2. Polyethylene-like Glass Transition (α_{PE}) within the Alkyl Nanodomains

The α_{PE} process in higher poly(*n*-alkyl acrylates) (P*n*AA) and poly(*n*-alkyl methacrylates) (P*n*AMA) is observed at lower temperatures besides the conventional glass transition involving the main chain (α) at higher temperature.[1,2] Dielectric, mechanical shear, and dynamic heat capacity relaxation spectroscopies were used for the observations. For dielectric spectroscopy, a commercial Novocontrol setup based on a Schlumberger SI1260 response analyzer was used to measure the complex dielectric function $\epsilon^*(\omega) = \epsilon' - i\epsilon''$ in the frequency range from 0.1 Hz to 1 MHz. Relaxation frequencies are taken from Havriliak−Negami (HN) fits ($\epsilon^*(\omega) = \Delta\epsilon(1 + (i\omega/\omega_{\mathrm{HN}})^b)^{-g} + \epsilon_\infty$) to the data. Peak maximum frequencies $\omega_{\max}$ and relaxation times τ given below were calculated according to $\omega_{\max} = \tau^{-1} = \omega_{\mathrm{HN}}\{\sin[\pi bg/(2g + 2)]/\sin[\pi b/(2g + 2)]\}^{-1/b}$. If required, an additional conductivity term $\sigma \sim \omega^{-1}$ was included. The complex shear modulus $G^*(\omega) = G' + iG''$ was measured in the frequency range from 1 to 100 rad s^{-1} with a Rheometrics Scientific RDAII instrument. The dynamic heat capacity $c_p^*(\omega,T) = c_p' - ic_p''$ (where c_p' and c_p'' are the real and imaginary parts, respectively) measurements were performed using a noncommercial setup of the 3ω method in the frequency range (0.2−2000 Hz). Details of the experimental setup and data evaluation are described elsewhere.[17]

Evidence for the interpretation that the α_{PE} process in higher P*n*AA and P*n*AMA is a polyethylene-like glass transition come from[1,2] (i) the Vogel−Fulcher-like temperature dependence of the α_{PE} relaxation time, $\tau_{C,\mathrm{PE}}$, obtained from the various relaxation spectroscopies (examples of P*n*AA for $C = 8$ and 10 and of P*n*AMA for $C = 7$ and 10 are shown in Figures 1 and 2, respec-

10.1021/ma048645x CCC: $27.50

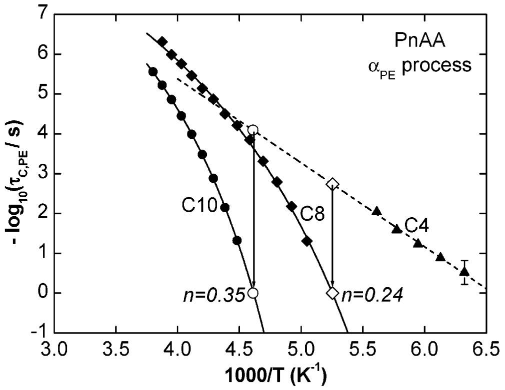

Figure 1. Arrhenius plot for the relaxation times $\tau_{C,\mathrm{PE}}$ of α_{PE} processes in higher P*n*AA with $C = 4$ (filled triangles), $C = 8$ (filled diamonds), and $C = 10$ (filled circles) as obtained from dielectric spectroscopy.[1] The lines are fits to the Vogel−Fulcher−Tammann−Hesse equation for $C = 8$ and $C = 10$ and a fit to the Arrhenius equation for $C = 4$. For explanation of the other symbols and vertical arrows, see text.

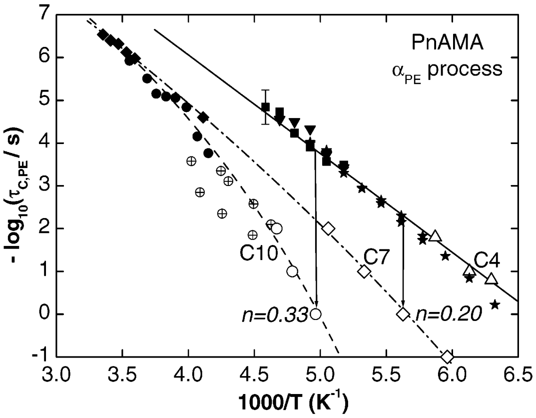

Figure 2. Arrhenius plot for the relaxation times $\tau_{C,\mathrm{PE}}$ of α_{PE} processes in higher P*n*AMA with $C = 4$ (triangles), $C = 7$ (diamonds), and $C = 10$ (circles). P*n*BMA ($C = 4$) samples with different degrees of polymerization (■, △, 1000; ▼, 52; ★, 18) are studied;[28] the P*n*AMA samples with $C = 7$ and $C = 10$ have high molecular weight ($P > 1000$, for details see ref 2). Data from dielectric spectroscopy (full symbols), shear spectroscopy (open symbols), and heat capacity spectroscopy (⊕) are shown. The lines are fits to the Vogel−Fulcher−Tammann−Hesse equation for $C = 7$ and $C = 10$ and a fit to the Arrhenius equation for $C = 4$. For explanation of the vertical arrows, see text.

tively). (ii) The α_{PE} process of poly(*n*-decyl methacrylate) ($C = 10$) was also observed[18] in the dynamic heat capacity, which is the hallmark of structural relaxation process. (iii) The α_{PE} process becomes increasing cooperative with the size of the alkyl nanodomain or increasing *C*, a trend that can be inferred from the concomitant increase of steepness index ("fragility"),[19] $m(C) = \mathrm{d}(\log\tau_{C,\mathrm{PE}})/\mathrm{d}(T_{\mathrm{ref}}/T)$ evaluated at $T = T_{\mathrm{ref}}$, where T_{ref} is the relaxation temperature at a fixed reference relaxation time $\tau_{C,\mathrm{PE}}(\mathrm{ref})$, which was chosen[1] to be 10^{-1} s. (iv) Also, there is observed increase of the shear mechanical intensity of the α_{PE} process with the volume fraction of alkyl groups.[20] The results altogether suggest that, in the higher members ($C \geq 6$) of both P*n*AA and P*n*AMA, the α_{PE} process is a cooperative glass transition within small alkyl nanodomains with size ≤ 2 nm.

The butyl members of the P*n*AA and P*n*AMA series, namely P*n*BA and P*n*BMA, having the shortest side chain ($C = 4$, with the smallest alkyl nanodomain size ≈ 0.5 nm), seem to be the exceptions. Their α_{PE} processes have properties different from that of the higher P*n*AA and P*n*AMA members. The α_{PE} process in P*n*BA or P*n*BMA has small intensity, its relaxation time, $\tau_{4,\mathrm{PE}}$, has nearly Arrhenius temperature dependence (see Figures 1 and 2), and its steepness (fragility) index *m* of about 14 for $\tau_{4,\mathrm{PE}}(\mathrm{ref}) = 10^{-1}$ s. The Arrhenius fit to the $\tau_{4,\mathrm{PE}}$ data of P*n*BA in Figure 1, for example, is given by the expression

$$\tau_{4,\mathrm{PE}} \approx 10^{-13.8} \exp(40.3\ \mathrm{kJ}/RT) \tag{1}$$

which has a physically interpretable prefactor. These features all seem to indicate that cooperativity is totally removed in the α_{PE} process of P*n*BA and P*n*BMA. As suggested before,[1] this happens because the nanodomain sizes of the α_{PE} process in P*n*BA and P*n*BMA are smaller than the cooperative length scale previously determined by multidimensional NMR experiments[21] slightly above T_g of other glass-formers.

3. Johari−Goldstein *β*-Relaxation in the Alkyl Nanodomains

We can show with the help of the coupling model[12−16] that the inferred vanishing cooperativity of the α_{PE} process in P*n*BA or P*n*BMA suggests that it is a secondary relaxation of the Johari−Goldstein kind, according to the definition given by a recent classification of secondary relaxations.[11] In the coupling model (CM), the relaxation time τ_{JG} of the supposedly universal Johari−Goldstein (JG) secondary relaxation has been identified with the independent relaxation time[11−16] τ_0, i.e.

$$\tau_0(T) \approx \tau_{\mathrm{JG}}(T) \tag{2}$$

There is support of this identification from experimental data of many bulk glass-formers,[11−13,22−24] which enable τ_0 to be calculated from the primary relaxation time τ_α by the familiar relation of the CM

$$\tau_\alpha = ({t_c}^{-n}\tau_0)^{1/(1-n)} \tag{3}$$

Here *n* is the coupling parameter that appears in the stretch exponent of the Kohlrausch function

$$\phi(t) = \exp[-(t/\tau_\alpha)^{1-n}] \tag{4}$$

used to fit the time dependence of the α-relaxation. The CM is based on the crossover from independent relaxation to Kohlrausch relaxation in a small neighborhood of time near t_c, from which eq 3 follows as a consequence. The existence of the crossover has been shown by the solutions of simplified models[14] and found experimentally by quasi-elastic neutron scattering experiments.[16,25] This issue will be further elucidated in the Discussion section, in conjuction with the other role played by the independent relaxation in eq 2. The crossover time t_c in eq 3, as determined directly by experimental data, has the approximate value of 2×10^{-12} s for conventional polymeric and small molecular glass-formers.[16,25] On combining eqs 2 and 3, we have the relation

$$\tau_\alpha \approx ({t_c}^{-n}\tau_{\mathrm{JG}})^{1/(1-n)} \tag{5}$$

between τ_α and τ_{JG}. Vanishing cooperativity of the α_{PE} process in P*n*BA or P*n*BMA is equivalent in the coupling model to reducing the coupling parameter *n* to zero value.[26] From eq 5, it follows that $\tau_\alpha = \tau_{\rm JG}$, and the α-relaxation and the JG relaxation become one and the same process. Specializing to the $\alpha_{\rm PE}$ process in P*n*BA or P*n*BMA, where τ_α is just $\tau_{4,\rm PE}$ and $\tau_{\rm JG}$ is $\tau_{4,\rm JG}$, we have

$$\tau_{4,\rm PE} \approx \tau_{4,\rm JG} \tag{6}$$

which indicates that the $\alpha_{\rm PE}$ process of P*n*BA or P*n*BMA ($C = 4$) and its associated JG relaxation are essentially one and the same process.

Thus, the data of the $\alpha_{\rm PE}$ processes in the P*n*AA and P*n*AMA series start out as a localized JG relaxation in the small (<1 nm) alkyl nanodomains of P*n*BA or P*n*BMA ($C = 4$). As C increases, the $\alpha_{\rm PE}$ process becomes progressively more cooperative in the larger (≥1 nm) alkyl nanodomains, and its characteristics are increasing different from that of JG relaxation. The characteristics include the Vogel–Fulcher-like temperature dependence of its relaxation time, $\tau_{C,\rm PE}$

$$\tau_{C,\rm PE} = A \exp\left(\frac{B}{T - T_0}\right) \tag{7}$$

and the larger steepness index m, defined with $\tau_{C,\rm PE}(\rm ref) = 10^{-1}$ s uniformly for all C. Since the JG relaxation is considered as a universal feature accompanying any primary relaxation, the JG relaxation of the $\alpha_{\rm PE}$ process should exist also in the higher members of the P*n*AA or P*n*AMA series. JG relaxation has not been resolved from the dielectric or mechanical spectra of P*n*AA or P*n*AMA with $C > 4$. Possibly this is due to overlap of the JG relaxation with the $\alpha_{\rm PE}$ process if $\tau_{\rm JG}$ is not much shorter than $\tau_{C,\rm PE}$, as we shall see in Figures 1 and 2 after the following point has been made.

The alkyl nanodomains of members of the P*n*AA series ($C \geq 4$) are all made of alkyl groups, with the length of the side chains and hence the size of the nanodomain being the only difference. Since the JG relaxation is a local process on the alkyl group, it does not change with the length of the side chain and should be the same for all members of the P*n*AA series ($C \geq 4$). The same remark applies to all members of the P*n*AMA series ($C \geq 4$). Hence, the unresolved JG relaxation ($\beta_{\rm PE}$) of P*n*AA and P*n*AMA with $C > 4$ can be identified with the $\alpha_{\rm PE}$ process in P*n*BA and P*n*BMA ($C = 4$), respectively. In particular, the JG relaxation time $\tau_{C,\rm JG}$ for any $C > 4$ can be taken as $\tau_{4,\rm JG}$ or $\tau_{4,\rm PE}$ by eq 6. Written out explicitly, we assume that

$$\tau_{C,\rm JG} = \tau_{4,\rm PE}, \quad \text{for } C > 4 \tag{8}$$

When applied to any $C > 4$, eq 2 takes the form of

$$\tau_{C,0} = \tau_{C,\rm JG} \tag{9}$$

where $\tau_{C,0}$ is the independent relaxation time of the alkyl nanodomain. This together with eqs 3, 5, and 8 combined lead to the relations

$$\tau_{C,\rm PE} = ({t_{\rm c}}^{-n_C}\tau_{C,0})^{1/(1-n_C)} = ({t_{\rm c}}^{-n_C}\tau_{C,\rm JG})^{1/(1-n_C)} = ({t_{\rm c}}^{-n_C}\tau_{4,\rm PE})^{1/(1-n_C)} \tag{10}$$

The first equality is basically the general eq 3 when applied to P*n*AA or P*n*AMA for $C > 4$. The second equality follows from the general relation between the independent relaxation time and the JG relaxation time (eq 2) when applied to P*n*AA or P*n*AMA for $C > 4$, i.e., $\tau_{C,0} \approx \tau_{C,\rm JG}$. The last equality is the consequence of the argument given in the beginning of this paragraph that the JG relaxation time $\tau_{C,\rm JG}$ for any $C > 4$ can be identified with $\tau_{4,\rm PE}$, i.e., eq 8.

The last relation

$$\tau_{C,\rm PE} = ({t_{\rm c}}^{-n_C}\tau_{4,\rm PE})^{1/(1-n_C)} \tag{11}$$

enables us to calculate the coupling parameters, n_C, and to predict the Kohlrausch exponent of the cooperative $\alpha_{\rm PE}$ process in any $C > 4$ member of P*n*AA and P*n*AMA from its $\alpha_{\rm PE}$ relaxation time $\tau_{C,\rm PE}$ and the $\alpha_{\rm PE}$ relaxation time $\tau_{4,\rm PE}$ in P*n*BA and P*n*BMA ($C = 4$), respectively. Before proceeding, we have to stipulate the limits of applicability of eq 9 and hence eq 11. The relaxation time of JG relaxation associated with cooperative α-relaxation invariably has Arrhenius temperature dependence in the glassy state. However, the Arrhenius temperature dependence no longer holds in the equilibrium liquid state,[23] where it is replaced by a stronger and possibly non-Arrhenius temperature dependence. In view of this, application of eqs 9–11 to $C > 4$ is limited to $\tau_{C,\rm PE}$ that are long, such that the corresponding temperature is near $T_{\rm g}$ of the $\alpha_{\rm PE}$ process.

In Figure 1, the relaxation times $\tau_{8,\rm PE}$ and $\tau_{10,\rm PE}$ of P*n*AA with $C = 8$ and $C = 10$, respectively, obtained from experiment are fit to the Vogel–Fulcher form and extended to lower temperatures. The open symbols on the Vogel–Fulcher fits mark the temperatures at which $\tau_{8,\rm PE}$ and $\tau_{10,\rm PE}$ have reached 1 s. We judge the value of 1 s for $\tau_{8,\rm PE}$ and $\tau_{10,\rm PE}$ is the best for calculating n_C with confidence because longer times obtained by the extrapolation involves larger uncertainty, and shorter times may invalidate using $\tau_{4,\rm PE}$ values determined by the Arrhenius temperature dependence given by eq 1. These $\tau_{4,\rm PE}$ values are shown by open symbols on the Arrhenius line in Figure 1 at the same temperatures as when $\tau_{8,\rm PE}$ and $\tau_{10,\rm PE}$ are equal to 1 s (as indicated by the two vertical arrows). With these values of $\tau_{4,\rm PE}$ corresponding to $\tau_{8,\rm PE} = 1$ s and $\tau_{10,\rm PE} = 1$ s, we calculate n_C for $C = 8$ and $C = 10$ by eq 11. The results are

$$n_8 = 0.24 \tag{12}$$

$$n_{10} = 0.35 \tag{13}$$

and, of course

$$n_4 = 0 \tag{14}$$

Similar analysis of the data of $\alpha_{\rm PE}$ in the P*n*AMA series is shown in Figure 2. The relaxation time, $\tau_{4,\rm PE}$, of P*n*BMA ($C = 4$, closed triangles) has an Arrhenius temperature dependence. On the other hand, the relaxation times $\tau_{7,\rm PE}$ and $\tau_{10,\rm PE}$ of P*n*AMA with $C = 7$ and $C = 10$, respectively, are non-Arrhenius, and the data are fit to the Vogel–Fulcher form and extended to lower temperatures. The two vertical arrows are located at temperatures where $\tau_{7,\rm PE}$ and $\tau_{10,\rm PE}$ have reached 1 s. The two corresponding $\tau_{4,\rm PE}$ values are determined by the intersections of the vertical arrow with the Arrhenius line representing $\tau_{4,\rm PE}$. The calculated values of n_C for $C = 7$ and $C = 10$ by eq 11 are

$$n_7 = 0.20 \tag{15}$$

and

$$n_{10} = 0.33 \tag{16}$$

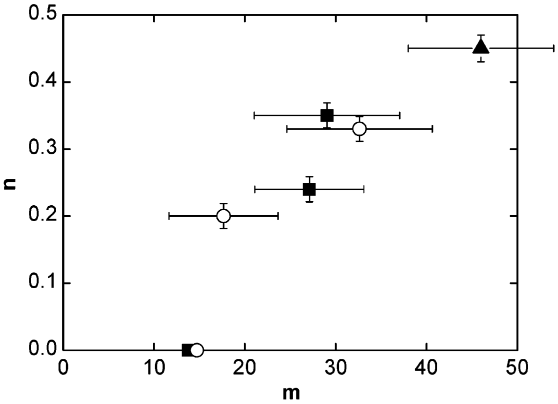

Figure 3. A cross-plot of n against m for $C = 4$, 8, and 10 of the PnAA series (■) and $C = 4$, 7, and 10 of the PnAMA series (○). The data point for amorphous PE (▲) is included.

For both the PnAA and PnAMA series, the deduced coupling parameters show that n_C increases with C or the alkyl nanodomain size. This behavior indicates from the coupling model interpretation that the molecular motions in the α_{PE} process become more intermolecularly coupled or more cooperative in the larger alkyl nanodomains. The same conclusion was drawn previously[1] from the increase of the steepness (fragility) index m with C. Therefore, our result derived from the CM, that n_C increases with C, leads to the same conclusion.

It was also shown in the previous work that m of the nanodomains are bounded by the steepness index of amorphous polyethylene (PE), estimated[27] to be ~46. For the same reason, we expect that n_C of the α_{PE} process in PnAA series is also bounded by the coupling parameter of amorphous PE. The latter is not exactly known because of lack of experimental data of amorphous PE. However, another estimate of its value may be obtained from that of polyisobutylene (PIB). The steepness index $m = \mathrm{d}(\log\tau_\alpha)/\mathrm{d}(T_{\mathrm{ref}}/T)$ of PIB is 45 for $\tau_\alpha(\mathrm{ref}) = 1$ s and 40 for $\tau_\alpha(\mathrm{ref}) = 10^{-1}$ s from mechanical relaxation data,[29] which is about the same as the value suggested for amorphous PE. There exists a strong correlation between n and m within the same class of glass-formers, PE and PIB in the present case. The coupling parameter of polyisobutylene is known,[29] and its value is 0.45. Thus, we may assume that the coupling parameter of amorphous PE has about the same value of 0.45. A cross-plot of n_C against $m(C) = \mathrm{d}(\log \tau_{C,\mathrm{PE}})/\mathrm{d}(T_{\mathrm{ref}}/T)$, with $\tau_{C,\mathrm{PE}}(\mathrm{ref}) = 10^{-1}$ s, for $C = 4$, 8, and 10 of the PnAA series and $C = 4$, 7, and 10 of the PnAMA series and amorphous PE is presented in Figure 3. The correlation between n_C and $m(C)$ is demonstrated.

4. Discussion and Conclusion

One of the goals of the present work is to make a case for the existence of the Johari−Goldstein (JG) secondary relaxation even in the alkyl nanodomains of the PnAA and PnAMA series. We also show that the ratio of the α_{PE} relaxation time to the JG relaxation time at temperatures near T_g is not very large (see Figures 1 and 2), consistent with the weak cooperativity of the α_{PE} process. The latter can be deduced from the low steepness (fragility) index and the smaller coupling parameter n of α_{PE}. In fact, for the larger nanodomains in $C = 10$, $m = 33$ and $n = 0.35$. As we have learned from the dielectric spectra of small molecular glass-formers with comparably smaller n such as glycerol ($n = 0.29$) and threitol ($n = 0.36$),[13] the JG relaxation is also not well separated from the much more intense α-relaxation and cannot be resolved at temperatures above T_g. The polymer 1,4-polyisoprene has a larger $n = 0.53$, but its JG relaxation was never resolved until recently only with the use of a highly sensitive dielectric relaxation instrument.[30] Thus, there is little hope of resolving the JG relaxation from α_{PE} for even the larger nanodomains in $C = 10$.

The Johari−Goldstein relaxation has been identified with the independent relaxation of the coupling model. The latter plays in the framework of this model two *separate* and *distinctive* roles at different time scales. At short times, when there are few independent relaxations present, they appear unconnectedly in space as localized motions just like the JG relaxation. Hence $\tau_0 \approx \tau_{JG}$, i.e., eq 2, and this is one role played by the independent relaxation. At times beyond τ_0 or τ_{JG}, more units can independently relax, they cannot be considered as isolated events anymore, and some degree of cooperativity (or dynamic heterogeneity) is required for motions to be possible. The degree of cooperativity and the corresponding length scale continue to increase with time as more and more units participate in the motion, as suggested by the evolution of dynamics of colloidal particles with time obtained by confocal microscopy.[31] These evolving processes contribute to the observed response at time longer than τ_0 or τ_{JG} and are responsible for the broad dispersion customarily identified as the JG relaxation by most workers. Within this definition of the JG relaxation, experiment performed to probe it will find that "essentially" all molecules contribute[32] to the JG relaxation, and the dynamics is dynamically and spatially heterogeneous as found by dielectric hole burning[33] and deuteron NMR experiments.[34] This remark may help to resolve the difference between two different points of view on the nature of the JG relaxation.[32,35]

After sufficiently long times, $t \gg \tau_0$ or τ_{JG}, *all* units attempt the independent relaxation, the *fully* cooperative relaxation regime with the largest cooperative length scale at that temperature is reached, and the averaged correlation function has the Kohlrausch's stretched exponential time dependence, eq 4. It is in this long time regime where the independent relaxation plays the other role described as follows. Not all attempted independent relaxation can succeed at the same time because of intermolecular interactions and constraints, resulting in *fully* heterogeneous cooperative dynamics with an average relaxation rate that can be time dependent and is smaller than the independent relaxation rate, τ_0^{-1}, at any time. The reduction of the average relaxation rate has to be considered on the basis of the independent relaxation rate, τ_0^{-1}. The CM interprets the stretched exponential correlation function to originate from slowing down of the independent relaxation rate τ_0^{-1} by the many-molecule dynamics. Specifically, τ_0^{-1} is replaced by a slower time-dependent averaged relaxation rate given by the *product* of τ_0^{-1} and $(\omega_c t)^{-n}$. The product form follows from the fact that all elementary attempts of molecular units to relax must have the characteristic rate given by τ_0^{-1}, and the many-body cooperative dynamics preventing attempts of molecules to be all successful merely slows down τ_0^{-1} by another multiplicative factor. Thus, the time-dependent rate has the product form, $\tau_0^{-1}f(t)$, where $f(t) < 1$. In particular, it has to be $\tau_0^{-1}(\omega_c t)^{-n}$ in order that the solution of the rate equation is the empirical Kohlrausch stretched exponential function (eq 4). As a bonus, the relation between τ_α and τ_0 given by eq 3 now comes out naturally as a consequence, after identifying ω_c introduced here by $\omega_c = (1 - n)^{-(1/n)}/t_c$. This is the other role played by the independent relaxation and its relaxation time τ_0, which makes connection with the α-relaxation time in the Kohlrausch correlation function. Experimentally, at high temperatures where all relaxation times become short, crossover of the independent relaxation to Kohlrausch relaxation directly at t_c was observed. The crossover determines the magnitude of t_c, which is about 2 ps for conventional polymers and molecular glass-formers.[16]

In the present work on relaxations in nanodomains of P*n*AMAs, the first role played by the independent relaxation with relaxation time $\tau_{C,0}$ is exemplified by eq 9. The second role it plays results in the first equality of eq 10. The second equality of eq 10 is obtained by combining the first part with eq 9. The last equality of eq 10 is generated after adopting the α_{PE} process of PnBMA ($C = 4$) as the JG relaxation of higher members of the P*n*AMA series ($C > 4$), i.e., eq 8. If n_C were known quantities, then the last equality, $\tau_{C,PE} = (t_c^{-n_C}\tau_{4,PE})^{1/(1-n_C)}$, offers a test of the CM application without any parameter. Unfortunately, the dielectric or mechanical relaxation data do not permit accurate determination of n_C because of the overlap of the α_{PE} relaxation with the α-relaxation of the main chain on the low-frequency side and its JG relaxation on the high-frequency side. In addition, there is probably a broadening caused by spatial heterogeneity of the confined nanodomains. Nevertheless, the values of n_C deduced from eq 11 are reasonable for polyethylene-like glass transition and support the increase of cooperativity of the α_{PE} relaxation with size of the nanodomain.

Acknowledgment. This work was supported by the Office of Naval Research and by the German Science Foundation (SFB 418).

References and Notes

(1) Beiner, M.; Huth, H. *Nature Mater.* **2003**, *2*, 595.
(2) Hiller, S.; Pascui, O.; Budde, H.; Kabisch, O.; Reichert, D.; Beiner, M. *New J. Phys.* **2004**, *6*, 10.
(3) Arrighi, V.; Triolo, A.; McEwen, I. J.; Holmes, P.; Triolo, R.; Amenitsch, H. *Macromolecules* **2000**, *33*, 4989.
(4) McCreight, K. W.; Ge, J. J.; Guo, M.; Mann, I.; Li, F.; Shen, Z.; Jin, X.; Harris, F. W.; Cheng, S. Z. *J. Polym. Sci., Part B: Polym. Phys.* **1999**, *37*, 1633.
(5) Nurulla, I.; Morikita, T.; Fukumoto, H.; Yamamoto, T. *Macromol. Chem. Phys.* **2001**, *202*, 2335.
(6) Chen, W.; Wunderlich, B. *Macromol. Chem. Phys.* **1999**, *200*, 283.
(7) Johari, G. P.; Goldstein, M. *J. Chem. Phys.* **1970**, *53*, 2372.
(8) Johari, G. P.; Goldstein, M. *J. Chem. Phys.* **1971**, *55*, 4245.
(9) Johari, G. P. *Ann. N.Y. Acad. Sci.* **1976**, *279*, 117.
(10) Johari, G. P.; Power, G.; Vij, J. K. *J. Chem. Phys.* **2002**, *116*, 5908.
(11) Ngai, K. L.; Paluch, M. *J. Chem. Phys.* **2004**, *120*, 857.
(12) Ngai, K. L. *J. Chem. Phys.* **1998**, *109*, 6982.
(13) Ngai, K. L. *J. Phys.: Condens. Matter* **2003**, *15*, S1107.
(14) Ngai, K. L.; Tsang, K. Y. *Phys. Rev. E* **1999**, *60*, 4511.
(15) Ngai, K. L. *IEEE Trans. Dielectr. Electron. Insul.* **2001**, *8*, 329.
(16) Ngai, K. L.; Rendell, R. W. In *Supercooled Liquids, Advances and Novel Applications*; Fourkas, J. T., Kivelson, D., Mohanty, U., Nelson, K., Eds.; ACS Symposium Series Vol. 676; American Chemical Society: Washington, DC, 1997; Chapter 4, p 45.
(17) Korus, J.; Beiner, M.; Busse, K.; Kahle, S.; Unger, R.; Donth, E. *Thermochim. Acta* **1997**, *304*−*305*, 99.
(18) Beiner, M.; Kabisch, O.; Reichl, S.; Huth, H. *J. Non-Cryst. Solids* **2002**, *307*−*310*, 658.
(19) Böhmer, R.; Ngai, K. L.; Angell, C. A.; Plazek, D. J. *J. Chem. Phys.* **1993**, *99*, 4201.
(20) Beiner, M.; Schröter, K.; Hempel, E.; Reissig, S.; Donth, E. *Macromolecules* **1999**, *32*, 6278.
(21) Tracht, U.; Wilhelm, M.; Heuer, A.; Feng, H.; Schmidt-Rohr, K.; Spiess, H. W. *Phys. Rev. Lett.* **1998**, *81*, 2727.
(22) Prevosto, D.; Capaccioli, S.; Lucchesi, M.; Rolla, P. A.; Ngai, K. L. *J. Chem. Phys.* **2004**, *120*, 4808.
(23) Paluch, M.; Roland, C. M.; Pawlus, S.; Ziolo, J.; Ngai, K. L. *Phys. Rev. Lett.* **2003**, *91*, 115701.
(24) Ngai, K. L.; Capaccioli, S. *Phys. Rev. E* **2004**, *69*, 031501.
(25) Colmenero, J.; Arbe, A.; Coddens, G.; Frick, B.; Mijangos, C.; Reinecke, H. *Phys. Rev. Lett.* **1997**, *78*, 1928.
(26) In bulk glass-formers, zero coupling parameter implies exponential correlation function, and vice versa. However, the confined nanodomains have additional spatial heterogeneity which contribute to distribution of relaxation times. Hence, vanishing cooperativity or zero coupling parameter does not imply exponential correlation function.
(27) Huang, D.; McKenna, G. B. *J. Chem. Phys.* **2001**, *114*, 5621.
(28) Reissig, S. Ph.D. Thesis, Universität Halle, Halle (Saale), Germany, 1999.
(29) Ngai, K. L.; Plazek, D. J.; Rizos, A. K. *J. Polym. Sci., Part B: Polym. Phys.* **1997**, *35*, 599.
(30) Roland, C. M.; Schroeder, M. J.; Fontanella, J. J.; Ngai, K. L. *Macromolecules* **2004**, *37*, 2630.
(31) Weeks, E. R.; Crocker, J. C.; Levitt, A.; Schofield, A.; Weitz, D. A. *Science* **2000**, *287*, 627.
(32) Vogel, M.; Rössler, E. *J. Chem. Phys.* **2000**, *114*, 5802.
(33) Richert, R. *Europhys. Lett.* **2001**, *54*, 767. Duvvuri, K.; Richert, R. *J. Chem. Phys.* **2003**, *118*, 1356.
(34) Böhmer, R.; Hinze, G.; Jörg, T.; Qi, F.; Sillescu, H. *J. Phys.: Condens. Matter* **2000**, *12*, A383.
(35) Johari, G. P. *J. Non-Cryst. Solids* **2002**, *307*−*310*, 317.

MA048645X